

**Magnetoresistance of mechanically stable Co nanoconstrictions**M. I. Montero,<sup>1,\*</sup> R. K. Dumas,<sup>1</sup> G. Liu,<sup>1</sup> M. Viret,<sup>1,2</sup> O. M. Stoll,<sup>1,2</sup> W. A. A. Macedo,<sup>1,3</sup> and Ivan K. Schuller<sup>1</sup><sup>1</sup>*University of California San Diego, Physics Department 0319, 9500 Gilman Drive, La Jolla, California 92093-0319, USA*<sup>2</sup>*Service de Physique de l'Etat Condensé, CEA Saclay, 91191 Gif sur Yvette Cedex, France*<sup>3</sup>*Laboratório de Física Aplicada, Centro de Desenvolvimento da Tecnologia Nuclear, 30123-970 Belo Horizonte, MG, Brazil*

(Received 30 July 2004; revised manuscript received 13 September 2004; published 12 November 2004)

We have studied the resistivity and magnetoresistance of mechanically stable Co contacts of nanometer sizes made by electron (e)-beam lithography on Si, GaAs, and Al<sub>2</sub>O<sub>3</sub> substrates. These constrictions were generated using two techniques. The first one uses conventional e-beam lithography to design fingers at different distances touching a perpendicular electrode. These contacts are generally in the tens of nanometers range with resistances as high as 500  $\Omega$ . After ion milling these contacts, resistances as high as 20 k $\Omega$  may be obtained. The second technique consists of Co deposition through a 400 nm hole made in a bilayer resist. The resistance in the “current perpendicular to the plane” geometry is monitored during deposition which is stopped when the desired resistance is obtained. Contacts in the k $\Omega$  range were thus fabricated between the bottom disk-like electrode and the top thin film. Magnetoresistance was measured in a wide range of applied magnetic fields and temperatures. Due to the large shape anisotropy difference between the electrodes, two well-defined coercive fields induce clear switching in the magnetization observable in the resistance. The magnetoresistances are in all cases below 1% and of varying signs. These effects are well within the range of the expected anisotropic magnetoresistance generated at the contacts or their vicinity.

DOI: 10.1103/PhysRevB.70.184418

PACS number(s): 75.75.+a, 75.47.Jn

**I. INTRODUCTION**

In the past years, the field of submicron scale ferromagnetic nanocontacts has gained great interest due to reports of extremely large values of magnetoresistance. This effect was observed in mechanically formed (contacting two separate wires glued in a simple piezoelectric device)<sup>1</sup> nanocontacts of various ferromagnetic metals,<sup>2,3</sup> half-metallic ferromagnets,<sup>4,5</sup> or electrodeposited nanocontacts.<sup>6–9</sup> Nanocontacts with resistances in the 5–1000  $\Omega$  range have been claimed to exhibit these large magnetoresistances.<sup>6,9</sup> The effect is attributed to ballistic magnetoresistance (BMR) and theoretical models based on the presence of an extremely thin domain wall at the nanocontact have been invoked to explain the effect.<sup>10–14</sup>

Although there are many interesting effects related to the electronic transport in ferromagnets in reduced dimensions, possible artifacts, such as magnetomechanical effects, have been ignored in this field until recently.<sup>15–17</sup> It is well known that the application of external fields on ferromagnetic materials induces forces which lead to displacements and distortions. Even when magnetic structures are expected not to move, i.e., are mechanically clamped, magnetostriction tends to distort ferromagnets in directions linked to their magnetization. Although the effect in simple ferromagnets is small (in the ppm range), it is likely to significantly affect the cross section of two electrodes in contact. Both magnetomechanical and magnetostrictive effects may be enhanced if the electrodes are macroscopic but the contacts are nanoscopic.

To exploit BMR in a device (i.e., to make it useful in a variety of applications), it is desirable to establish this effect in mechanically stable, lithographically defined structures. To the best of our knowledge, BMR has never been observed in rigid structures such as those obtained using lithographic techniques.<sup>15,18–22</sup>

In this paper we report the magnetotransport properties of mechanically stable magnetic nanoconstrictions prepared using two methods based on conventional e-beam lithography. In the first method, seven ferromagnetic “fingers” are placed at slightly different distances from a perpendicularly oriented main ferromagnetic electrode. In this way, we are able to produce ferromagnetic nanoconstrictions with various widths in a single sample. The second method consists of the deposition of a pillar of magnetic material through a nanometer scale hole made in a resist bilayer.

**II. EXPERIMENT**

Co nanoconstrictions with different widths on a single substrate were simultaneously prepared using e-beam lithography and ion milling. The fabrication process consists of three separate stages. In the first stage, a 50 nm thick Co film is deposited onto Si, GaAs, and/or Al<sub>2</sub>O<sub>3</sub> substrates by molecular beam epitaxy, subsequently a 3 nm Al capping layer is grown to prevent the oxidation of the Co film. In the second stage, a polymethylmethacrylate (PMMA) layer is spun onto the Co film, then the pattern for the nanoconstrictions is defined using e-beam writing. The essential parts of the e-beam pattern are seven finger-like contact structures in the middle of the pattern and a perpendicularly oriented common central electrode. Each of the fingers has a width of 1.2  $\mu\text{m}$  whereas the central electrode is 4  $\mu\text{m}$  wide. The perpendicular orientation together with the different widths ensures different coercive fields of the finger and the central electrode. The nanoconstrictions are obtained using a single scan with the electron beam, which produces a cut between the common electrode and the fingers. After the e-beam writing the PMMA structure is transferred into the magnetic film by ion milling, followed by a lift-off process. In the final

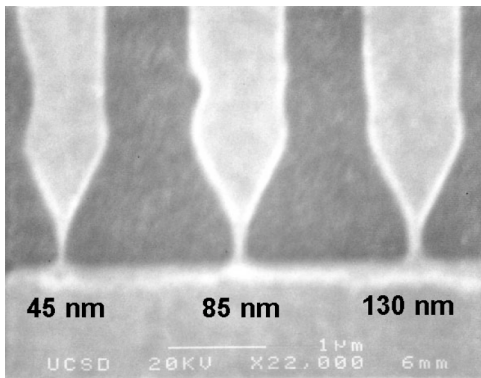


FIG. 1. Scanning electron micrograph of three typical nanoconstrictions with different widths on a Co film on Si. The width decreases from 130 nm on the right to 45 nm on the left.

stage, macroscopic contacts are defined using standard optical lithography and Ar-sputter etching for the transport measurements.

Figure 1 shows three typical nanoconstrictions with different widths ranging from 45 nm to over 130 nm in a Co film on Si. The nanolithographic process has been tested on many samples. Although the width of the bridges cannot be accurately predicted, the process gives reproducible results in the sense that there is always a usable series of nanoconstrictions with widths in the range of 30–150 nm.

A second type of magnetic nanoconstrictions was prepared depositing a pillar of Co through a nanometer scaled hole made in a resist bilayer (see Fig. 2). First, a conducting base layer is deposited on a Si substrate. The base layer is created using direct current magnetron sputtering. A 10 nm Al layer is sputtered on an undoped Si substrate to improve the adhesion of the 30 nm Au layer. A 200 nm methacrylic acid (MAA) resist layer is spun on the sample, and a 100 nm PMMA layer is spun on the MAA layer. The sample is baked for 1 h at 155 °C before undergoing e-beam lithography in which a circle is written into the bilayer resist. The sample is developed to remove the exposed resist creating a hole (around 400 nm diameter) through to the conducting base layer. In the final step, Co is deposited by e-beam evaporation. During the evaporation a Co pillar is grown in the cylindrical well created in the resist layers. At some point during evaporation the growing pillar and the Co layer on top of

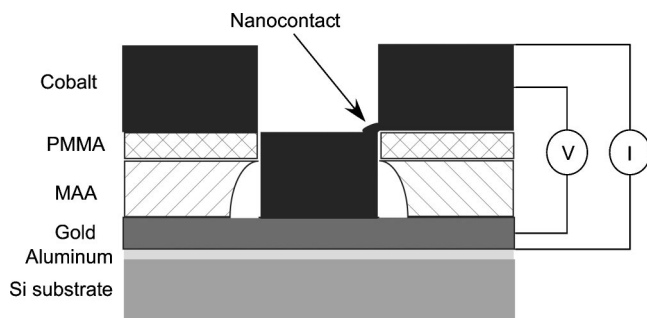


FIG. 2. Preparation of nanoconstriction using a hole in an insulating membrane while monitoring the resistance during growth of a Co nanopillar.

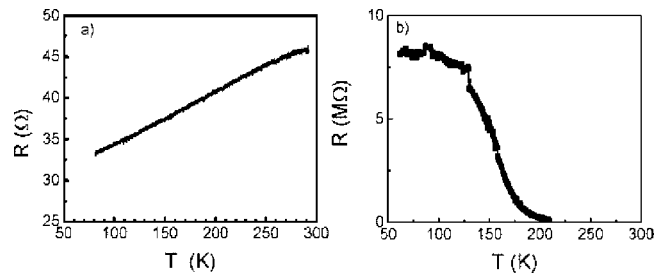


FIG. 3. Evolution of the resistance with temperature for (a) a 75 nm Co nanoconstriction and (b) 120 nm nanogap on GaAs.

the resist layer make contact which creates a nanoconstriction. The resistance in the “current perpendicular to the plane” geometry is monitored during the deposition, which is stopped when a desired resistance is obtained. Contacts in the kΩ range can thus be reproducibly fabricated between the bottom disk-like electrode and the top thin film.

Transport measurements were done using a four-point technique in a wide temperature range (4.2–300 K) up to 80 kG with the applied magnetic field parallel to the film plane.

### III. RESULTS

The temperature dependence of the resistance allows discriminating between the nanogaps and nanoconstrictions even if the nanoconstrictions or nanogaps are below the resolution of the scanning electron microscopy (see Fig. 3).

As an illustration of many measurements we present results for a sample consisting of a 50 nm Co film on Si with four nanoconstrictions of widths approximately 30, 40, 50, and 100 nm. Figure 4(a) shows typical magnetoresistance curves for three nanoconstrictions at  $T=4.2$  K when the applied magnetic field is in the film plane and perpendicular to the “fingers.” The magnetic field was swept from 2 to  $-2$  kOe. A peak was observed at  $-45$  Oe close to the coercive field for the three nanoconstrictions. In all the cases the magnetoresistances are around 0.2%, close to the magnetoresistances obtained in Co nanowires,<sup>23</sup> NiFe nanocontacts,<sup>18</sup> and Ni nanoconstrictions.<sup>24</sup> The magnetoresistance (MR) for these three contacts have the same magnitude up to 300 K [see Fig. 4(b)]. In this geometry the MR is almost indepen-

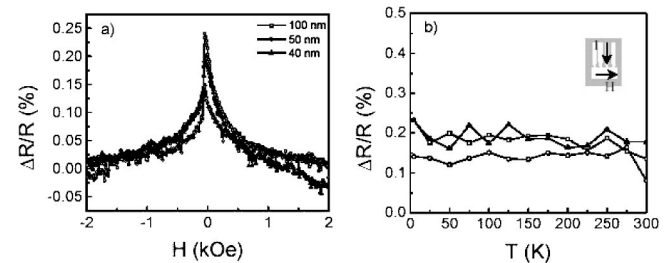


FIG. 4. (a) Magnetoresistance of three nanoconstrictions (100, 50, and 40 nm width) with the magnetic field in the film plane and perpendicular to the nanoconstrictions, at 4.2 K (field swept from positive to negative). (b) Evolution of the magnetoresistance with temperature for the three nanoconstrictions.

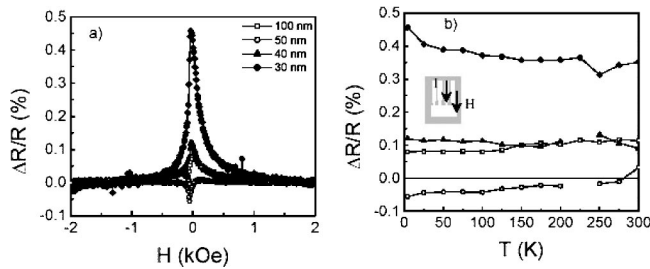


FIG. 5. (a) Magnetoresistance of four nanoconstrictions (100, 50, 40, and 30 nm width) obtained with the magnetic field in the film plane and parallel to the nanoconstrictions, at 4.2 K (field swept from positive to negative). (b) Evolution of the magnetoresistance with temperature for the four nanoconstrictions.

dent of the temperature and nanoconstriction size in all ranges investigated.

With the magnetic field applied parallel to the fingers, the magnetoresistances remain below 1% for the four nanoconstrictions (see Fig. 5). However, they behave differently depending on the nanoconstriction width. The 30 and 40 nm nanoconstrictions exhibit a positive MR peak at  $-35$  Oe almost temperature independent in the range of temperatures up to 300 K. The 50 nm nanoconstriction exhibits a negative MR dip at  $-55$  Oe. The depth of the dip decreases with the temperature until it disappears above 275 K, while a peak at 65 Oe develops with increasing temperature. This peak is the only feature present at temperatures above 275 K. The 100 nm nanoconstriction shows a peak at  $-5$  Oe and a dip at  $-65$  Oe. Again, the depth of the dip decreases with the temperature until it disappears above 275 K.

All nanoconstrictions with sizes in the 30–150 nm range, prepared by this method, have less than 1% magnetoresistances. To narrow the nanoconstriction width we performed an additional ion milling while monitoring its resistance. Figure 6(a) shows the resistance versus applied magnetic field for a 150 nm Co nanoconstriction. The measurements were taken at  $T=4.2$  K with the magnetic field parallel to the film and perpendicular to the nanoconstriction. The curve shows a slight MR of less than 0.02%. After ion milling the sample a second time, the resistance increases substantially, the nanoconstriction is narrower (less than 30 nm width) while the MR increases only up to 0.4% [see Fig. 6(b)]. Resistances as high as 23 k $\Omega$  were obtained for some contacts which at these very high resistances exhibited a negative coefficient of

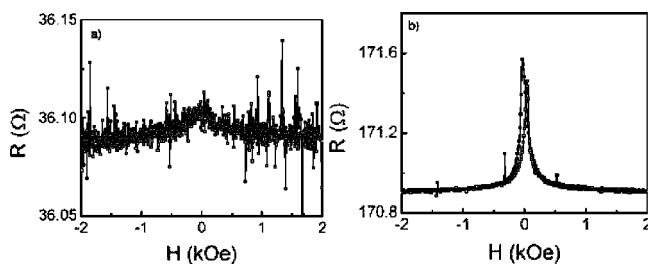


FIG. 6. Magnetoresistance of a 150 nm nanoconstriction before (a) and after (b) a second ion milling process. Both curves were obtained with the magnetic field in the film plane and parallel to the nanoconstrictions, at 4.2 K (both field direction sweeps).

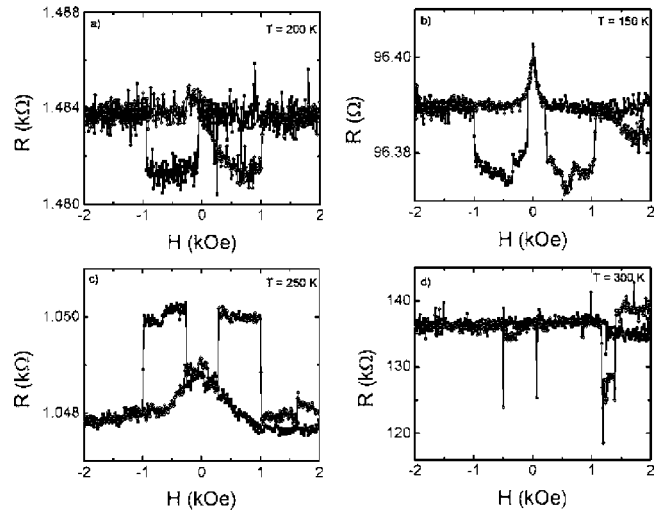


FIG. 7. Magnetoresistance of a pillar nanoconstriction (a) initial state, (b) after one day, (c) after three days and (d) after running a large current through the sample. All curves were obtained with the magnetic field parallel to the film plane.

resistivity and again small magnetoresistance.

All the nanoconstrictions prepared by patterning the Co film show very small values of magnetoresistance with resistances up to 500  $\Omega$ . After a second ion mill the nanoconstrictions yield resistances in the 20 k $\Omega$  range, but still the magnetoresistances were less than 1%. The nanoconstrictions prepared on GaAs or Al<sub>2</sub>O<sub>3</sub> substrates yield similar results.

Resistances in the k $\Omega$  range were obtained by depositing a Co pillar through a nanometer hole made in a bilayer resist (as described in Sec. II). Figure 7 shows the time evolution of the magnetoresistance of a nanoconstriction with an initial resistance of 1.5 k $\Omega$  [see Fig. 7(a)] a magnetic field parallel to the film at 200 K. Two distinct changes in resistance were found corresponding to the two different coercive fields of the top and bottom electrodes. Changes in resistance of the order of 0.2% were observed. While taking measurements at 4.2 K, a sudden large drop in the resistance to about 96  $\Omega$  occurred. This 96  $\Omega$  resistance was quite stable for a few days, [see Fig. 7(b)] where the 150 K magnetoresistance curve includes two distinct drops at the coercive fields as well as a small peak around zero field. With the sample kept in the cryostat for two days, the resistance jumped back up to around 1 k $\Omega$  [see Fig. 7(c)]. With this sudden change in resistance came a different magnetoresistive behavior. There were still two distinct jumps (occurring at roughly the same coercive fields as in the initial state) but now they were positive and not negative as earlier. The following two days no further changes in MR or resistance were observed. Finally, a large current was run through the sample to increase the resistance roughly to 136 k $\Omega$ . However, no magnetoresistive effects were observed at this resistance [see Fig. 7(d)].

#### IV. DISCUSSION

The results showed above can be interpreted as due to anisotropic magnetoresistance (AMR) together with single domain wall resistance. For the patterned nanoconstrictions,



when the magnetic field is applied parallel to the fingers and to the current, the AMR ratio is 0.33%, 0.25%, and 0.64% for the 100, 50, and 40 nm nanoconstrictions, respectively. Therefore the measured resistance changes ( $\Delta R/R$ ) are within the expected AMR contributions. Note that in our case the current flows perpendicular in some portions of the sample and parallel in others. Moreover, due to the existence of the nanoconstrictions, a complicated domain structure maybe expected and is found in its vicinity. Therefore, if the magnetoresistance is caused by ordinary anisotropic MR, in our case this will be a mixture of parallel and perpendicular MR.<sup>25</sup> For the 100 and 50 nm nanoconstrictions, the magnetoresistance curves also show a dip around  $-65$  Oe, which can be attributed to individual domain wall resistance. It has been reported that domain wall resistance effects can be positive<sup>26–29</sup> or negative<sup>30,31</sup> in good agreement with theoretical models. Domain walls may suppress weak localization,<sup>12</sup> thereby removing a source of resistivity, while band bending effects<sup>32</sup> imply either negative or positive magnetoresistance. Theoretical predictions<sup>12,33</sup> also imply that the domain wall resistance decreases with increasing temperature. In our case, the negative magnetoresistance decreases with increasing temperature, until only AMR is observed at temperatures above 275 K.

In the case of the “pillar” nanoconstrictions, the negative (positive) jump at  $-100$  Oe ( $-260$  Oe) can be interpreted as an injection and trapping of a domain wall and the positive (negative) jump at  $-1000$  Oe ( $-1000$  Oe) as a depinning and annihilation of the domain wall. Again a magnetoresistance

less than 0.2% can be explained by the AMR of the nanoconstriction.

## V. CONCLUSIONS

To summarize, we have developed two methods to prepare mechanically stable magnetic nanoconstrictions. Using standard e-beam lithography in combination with dry etching we are able to fabricate reproducible Co nanoconstrictions with widths in the range of 30–150 nm and resistances as high as 500  $\Omega$ . Ion milling allows increasing the resistances of these constrictions in the 20 k $\Omega$  range. The second technique consists of Co deposition through a nanoscale hole made in a bilayer resist. Contacts in the k $\Omega$  range were thus fabricated between the bottom disk-like electrode and the top thin film. The transport properties of both types of nanoconstrictions have been measured and values of magnetoresistance of less than 1% were obtained between 4.2 and 300 K and for constrictions with resistance as high as 135 k $\Omega$ . These effects are well within the range of the expected AMR generated at the contacts or their vicinity.

## ACKNOWLEDGMENTS

This work was supported by the US AFOSR-MURI. O.M.S. acknowledges financial support from the Deutscher Akademischer Austauschdienst (DAAD). W.A.A.M. acknowledges support from CNPq (Brazil).

\*Author to whom correspondence should be addressed; FAX: 858-534-0173; Electronic address: mmontero@ucsd.edu

<sup>1</sup>J.L. Costa-Krämer, N. García, P. García-Mochales, P.A. Serena, M.I. Marqués, and A. Correia, *Phys. Rev. B* **55**, 5416 (1997).

<sup>2</sup>N. García, M. Muñoz, and Y.-W. Zhao, *Phys. Rev. Lett.* **82**, 2923 (1999).

<sup>3</sup>N. García, M. Muñoz, V.V. Osipov, E.V. Ponzovskaya, G.G. Qian, I.G. Saveliev, and Y.-W. Zhao, *J. Magn. Magn. Mater.* **240**, 92 (2002).

<sup>4</sup>J.J. Versluijs, M.A. Bari, and J.M.D. Coey, *Phys. Rev. Lett.* **87**, 026601 (2001).

<sup>5</sup>S.H. Chung, M. Muñoz, N. García, W.F. Egelhoff, Jr., and R.D. Gomez, *Phys. Rev. Lett.* **89**, 287203 (2002).

<sup>6</sup>N. García, M. Muñoz, G.G. Qian, H. Rohrer, I.G. Saveliev, and Y.-W. Zhao, *Appl. Phys. Lett.* **79**, 4550 (2001).

<sup>7</sup>N. García, G.G. Qian, and I.G. Saveliev, *Appl. Phys. Lett.* **80**, 1785 (2002).

<sup>8</sup>H.D. Chopra and S.Z. Hua, *Phys. Rev. B* **66**, 020403(R) (2002).

<sup>9</sup>S.Z. Hua and H.D. Chopra, *Phys. Rev. B* **67**, 060401(R) (2003).

<sup>10</sup>K. Nakanishi and Y.O. Nakamura, *Phys. Rev. B* **61**, 11278 (2000).

<sup>11</sup>G. Tatara, Y.-W. Zhao, M. Muñoz, and N. García, *Phys. Rev. Lett.* **83**, 2030 (1999).

<sup>12</sup>G. Tatara and H. Fukuyama, *Phys. Rev. Lett.* **78**, 3773 (1997).

<sup>13</sup>P. Bruno, *Phys. Rev. Lett.* **83**, 2425 (1999).

<sup>14</sup>Y. Labaye, L. Berger, and J.M.D. Coey, *J. Appl. Phys.* **91**, 5341

(2002).

<sup>15</sup>M. Gabureac, M. Viret, F. Ott, and C. Fermon, *Phys. Rev. B* **69**, 100401(R) (2004).

<sup>16</sup>E.B. Svedberg, J.J. Mallet, H. Ettetdgui, G. Li, P.J. Chen, A.J. Shapiro, T.P. Moffat, and W.F. Egelhoff, Jr., *Appl. Phys. Lett.* **84**, 236 (2004).

<sup>17</sup>W.F. Egelhoff, Jr., L. Gan, H. Ettetdgui, Y. Kadmon, C.J. Powell, P.J. Chen, A.J. Shapiro, R.D. McMichael, J.J. Mallet, T.P. Moffat, M.D. Stiles, and E.B. Svedberg, *J. Appl. Phys.* **95**, 7554 (2004).

<sup>18</sup>K. Miyake, K. Shigeto, K. Mibu, T. Shinjo, and T. Ono, *J. Appl. Phys.* **91**, 3468 (2002).

<sup>19</sup>G. Dumpich, T.P. Krome, and B. Hausmanns, *J. Magn. Magn. Mater.* **248**, 241 (2002).

<sup>20</sup>I.L. Prejbeanu, M. Viret, L.D. Buda, U. Ebels, and K. Ounadjela, *J. Magn. Magn. Mater.* **240**, 27 (2002).

<sup>21</sup>M. Viret, S. Berger, M. Gabureac, F. Ott, D. Olligs, I. Petej, J.F. Gregg, C. Fermon, G. Francinet, and G. Le Goff, *Phys. Rev. B* **66**, 220401(R) (2002).

<sup>22</sup>I.V. Roshchin, J. Yu, A.D. Kent, G.W. Stupian, and M.S. Leung, *IEEE Trans. Magn.* **37**, 2101 (2001).

<sup>23</sup>B. Hausmanns, T.P. Krome, G. Dumpich, E.F. Wassermann, D. Hinzke, U. Nowak, and K.D. Usadel, *J. Magn. Magn. Mater.* **240**, 297 (2002).

<sup>24</sup>O. Ozatay, P. Chalsani, N.C. Emley, I.N. Krivorotov, and R.A. Buhrman, *J. Appl. Phys.* **95**, 7315 (2004).

- <sup>25</sup>T.R. McGuire and R.I. Potter, *IEEE Trans. Magn.* **11**, 1018 (1975).
- <sup>26</sup>M. Viret, D. Vignoles, D. Cole, J.M.D. Coey, W. Allen, D.S. Daniel, and J.F. Gregg, *Phys. Rev. B* **53**, 8464 (1996).
- <sup>27</sup>D. Ravelosona, A. Cebollada, F. Briones, C. Diaz-Paniagua, M.A. Hidalgo, and F. Batallan, *Phys. Rev. B* **59**, 4322 (1999).
- <sup>28</sup>M. Viret, Y. Samson, P. Warin, A. Marty, F. Ott, E. Sondergard, O. Klein, and C. Fermon, *Phys. Rev. Lett.* **85**, 3962 (2000).
- <sup>29</sup>R. Danneau, P. Warin, J.P. Attané, I. Petej, C. Beigné, C. Fermon, O. Klein, A. Marty, F. Ott, Y. Samson, and M. Viret, *Phys. Rev. Lett.* **88**, 157201 (2002).
- <sup>30</sup>U. Ruediger, J. Yu, S. Zhang, A.D. Kent, and S.S.P. Parkin, *Phys. Rev. Lett.* **80**, 5639 (1998).
- <sup>31</sup>S.J.C.H. Theeuwen, J. Caro, K.I. Schreurs, R.P. van Gorkom, K.P. Wellock, N.N. Gribov, S. Radelaar, R.M. Jungblut, W. Oepts, R. Coehoorn, and V.I. Kozub, *J. Appl. Phys.* **89**, 4442 (2001).
- <sup>32</sup>R.P. van Gorkom, A. Brataas, and G.E.W. Bauer, *Phys. Rev. Lett.* **83**, 4401 (1999).
- <sup>33</sup>Y. Lyanda-Geller, I.L. Aleiner, and P.M. Goldbart, *Phys. Rev. Lett.* **81**, 3215 (1998).